NÖHÜ Müh. Bilim. Derg. / NOHU J. Eng. Sci., 2021; 10(2), 791-799

Niğde Ömer Halisdemir Üniversitesi Mühendislik Bilimleri Dergisi
Niğde Ömer Halisdemir University Journal of Engineering Sciences

Araştırma makalesi / Research article

www.dergipark.org.tr/tr/pub/ngumuh / www.dergipark.org.tr/en/pub/ngumuh

A similarity approach to boundary layer equations of a non-Newtonian fluid: Carreau-Yasuda model

Bir non-Newtonyen akışkanının sınır tabakası denklemleri için benzerlik yaklaşımı: Carreau-Yasuda modeli

Yiğit Aksoy[1,*], Hikmet Sümer[2], Kıvanç Samra[3]

[1,2,3]*Manisa Celal Bayar University, Mechanical Engineering Department, 45140, Manisa, Turkey*

Abstract

The present study considers a non-Newtonian flow over a horizontally immersed flat plate kept at a different temperature relative to the fluid. An inviscid free stream with uniform velocity induces the flow over the plate where an incompressible boundary layer viscously occurs. It is stipulated that the fluid obeys the Carreau-Yasuda constitutive equation. Analytical investigations begin with the derivation of momentum and energy equations followed by boundary layer simplifications. Scaling symmetries are subsequently calculated to define similarity variables to transform boundary layer equations into ordinary differential forms. Later, solutions of the governing equations are pursued by a numerical scheme based on finite differences. Thanks to those solutions, the effects of significant non-dimensional parameters, such as Deborah and Prandtl numbers, on both momentum and thermal boundary layers are examined throughout the figures. The Nusselt number's variation with non-dimensional numbers is also questioned for the study's heat transfer part.

Keywords: Non-newtonian fluids, Carreau fluid, Carreau-Yasuda fluid, Boundary layer flow, Similarity transformations.

Özet

Bu çalışmada, akışkana göre farklı bir sıcaklıkta ve yatay olarak yerleştirilmiş düz bir plaka üzerinde Newtonyan olmayan bir akış göz önüne alınmıştır. Sıkıştırılamaz, kararlı ve düzgün hıza sahip viskoz olmayan bir serbest akım plaka üzerinde viskoz bir sınır tabakası akışına neden olmaktadır. Newtonyen olmayan akışın Carreau-Yasuda akışkan modeline uyması öngörülmüştür. Analitik yaklaşım, momentum ve enerji denklemlerinin türetilmesi ve ardından sınır tabakası basitleştirmeleri ile başlar. Denklemlerin ölçekleme simetrileri kullanılarak hesaplanan benzerlik değişkenleri vasıtası ile kısmi diferansiyel denklem formunda olan sınır tabakası denklemleri adi forma indirgenmiştir. Daha sonra, Söz konusu denklemlerin sayısal çözümleri sonlu farklar algoritmasına dayanan sayısal bir çözümleyici ile bulunmuştur. Bu çözümler sayesinde, Deborah ve Prandtl sayıları gibi önemli boyutsuz parametrelerin hem momentum hem de termal sınır tabakası kalınlıkları üzerindeki etkileri grafikler üzerinden incelenmiştir. Ayrıca Nusselt sayısının boyutsuz sayılara göre değişimi de çalışmanın ısı transferi kısmı için araştırılmıştır.

Anahtar kelimeler: Newtonyen olmayan akışkan, Carreau akışkanı, Carreau-Yasuda akışkanı, Sınır tabakası akışı, Benzerlik dönüşümleri.

1 Introduction

Many fluids commonly possess a varying viscosity with shear rate and dissociate from Newtonian fluids of constant viscosity. Various mathematical models have been proposed to predict their flow for almost a century. Rather than more general non-Newtonian fluids, several fluids, such as ketchup, toothpaste, and blood that may obey these constitutive equations, are generalized Newtonian fluids [1]. Accordingly, unlike Newtonian fluid's constant viscosity, a generalized Newtonian fluid, briefly GNF, shall exhibit its viscosity, namely apparent viscosity, to either rise or decries under varying shear rate conditions. When the viscosity reduces with increasing shear rate, the fluid is called shear thinning, whereas shear-thickening for growing viscosity. Before getting started in mathematical aspects, we further remark that while increasing shear rate, the apparent viscosity ranges from an initial to a limit value, and between these values, each apparent viscosity has a unique curve. Excluding shear rates where initial viscosity is exceeded and limit viscosity values are reached, the fluid can exhibit Newtonian behavior, which indicates constant viscosity. However, the apparent viscosity solely alters in the transition zone, namely, the power-law zone, where the fluid exposes non-Newtonian behavior. A convenient mathematical model that can anticipate the zones in an optimum manner requires the least parameter to fit the viscosity data with a minimal deviation. In practice, however, only focusing on the power-law zone, the Oswalt-de-Waele model [2], i.e., power-law fluid, is frequently used due to its simple mathematical form as below:

$$\mu(|\dot{\gamma}|)=\eta|\dot{\gamma}|^{n-1} \tag{1}$$

* Sorumlu yazar / Corresponding author, e-posta / e-mail: yigit.aksoy@cbu.edu.tr (Y. Aksoy)
Geliş / Recieved: 14.12.2020 Kabul / Accepted: 30.03.2021 Yayımlanma / Published: 27.07.2021
doi: 10.28948/ngmuh.840284

where μ is the apparent viscosity, $|\dot{\gamma}|$ is the rate of deformation tensor, η is the consistency index and n is the power-law index. Since the apparent viscosity in the preceding formula is proportional to $n-1$ power of the shear rate, the fluid gets thinner as shear rate increases for $n<1$. Such fluids are called "shear thinning" as mentioned before, otherwise "shear thickening" for $n>1$. Although a viscous fluid must have a non-zero and finite viscosity at any shear rate, the power-law formula yields zero and infinite values for the apparent viscosity at very low and at very high shear rates, respectively. To overcome the shortcoming in question, numerous mathematical models, for instance, Cross [3], Sisko [4], Carreau [5], and Carreau-Yasuda [6], have emerged over the years to ensure the entire viscosity curve. For the rest of the study, we now pay our attention to the Carreau-Yasuda model by the equation:

$$\mu\left(|\dot{\gamma}|\right)=\mu_{\infty}+\left(\mu_{0}-\mu_{\infty}\right)\left(1+\lambda|\dot{\gamma}|^{m}\right)^{\frac{n-1}{m}} \tag{2}$$

In the equation above, μ_0 and μ_∞ are the limit viscosities at the very low and high enough shear rates, respectively, and n is power-law index as the former. Unlike the Oswalt-de-Waele model, Carreau-Yasuda requires secondary power-law exponent m that characterizes the curvature connecting the Newtonian plateau with the power-law region. λ the time constant, namely material relaxation time defines specific shear rates corresponding to boundaries of the power-law region in a viscosity-shear rate curve. GNF models lack molecular insight due to their strong empirical base but can roughly describe molecular weight dependence of viscosity by correlating the time constant with molecular structure. Note that when $m=2$, Equation (2) turns out to Carreau fluid model [5] moreover Newtonian fluid for $\lambda=0$.

Carreau-Yasuda and its predecessor have been extensively used in studies on non-Newtonian flow problems for recent years. For instance, a peristaltic flow of electrically conducting Carreau-Yasuda fluid induced by the peristaltic motion of a curved channel is examined under the influence of a magnetic field by Abbasi et al. [7]. Boyd and Buick [8] studied a blood-flow inside arteries and treated the blood as Carreau-Yasuda and Casson model compared to analogous Newtonian flows. Raju [9] et al. assessed Carreau, Ellis, and Cross models' applicability to polymeric materials' viscosity data. The study reveals that Carreau and Ellis are far ahead of the Cross model regarding the overall error in estimates of the non-Newtonian viscosity-shear rate relationship. Due to their ease of calculations, among non-Newtonian fluid models, GNF formulas, especially Carreau, Cross, and power-law models [10], are widely used in commercial software products such as Moldflow, Comsol, and Ansys.

Governing equations of a Newtonian fluid require powerful analytical or most likely numerical tools to analyze, and so do those of non-Newtonian fluids, of course. Therefore, numerical approaches are conventional for the solutions, albeit the need for supercomputers due to intensive matrix operations. In contrast, analytical solutions are more robust and reliable, nevertheless literally rare in the literature. As well as linearization procedures, logical simplifications on the equations can also be prerequisites for the analytical solutions. Thus, results are possibly approximate and limited; however, they are still necessary for the fundamental understanding and will be. As one of those and a systematic approach for ease of calculation, the boundary layer theory [11] recently draws keen attention, especially in non-Newtonian fluid flows over solid bodies. Boundary layer theory states that if the changes occur only in a narrow area, not all the factors affecting the problem may be necessary, so that some may be negligible. It is, therefore, a general guide that enables us to reach a more straightforward form of governing equations. While considering only conservation of momentum for flow over a flat plate, boundary layer equations of Carreau fluid are derived and solved numerically in [12]. The boundary layer approach yields partial differential equations ultimately, despite being quite simplifying. However, in most studies, unlike [12], transforming boundary layer equations into ordinary differential equation forms using similarity variables is preferred for ease of numerical calculations. For instance, Khan and Hashim [13] presented a stepwise study on Carreau fluid flow over a stretched sheet and obtained similarity solutions for both momentum and thermal boundary layer equations.

Similarity solutions necessitate new variables, namely similarity variables, which can transform boundary layer equations ultimately into relevant ordinary form. Although conventional forms of similarity are used in most studies, Lie group techniques detailed in [14] may unveil further by finding out invariants, i.e., symmetries, of the equations. Applications of Lie groups on non-Newtonian fluids, especially GNF, are given in [15-17] for consideration of readers. We intend to conduct an analytical study on a non-Newtonian fluid flow over a flat plate in light of previous studies. On account of studying the cooling of the cold plate, the heat transfer part of the problem is further considered in terms of non-dimensional parameters, especially the Nusselt number, which is engineering interest to evaluate. As the Carreau-Yasuda model holds for non-Newtonian behavior in the flow, we ignore viscous heating in the energy equation. We divide the study into the following sections, respectively; formulation of the problem, boundary layer analysis, similarity transformations, and finally, numerical solutions followed by comments of the results via figures.

2 Physical configuration and conservation laws

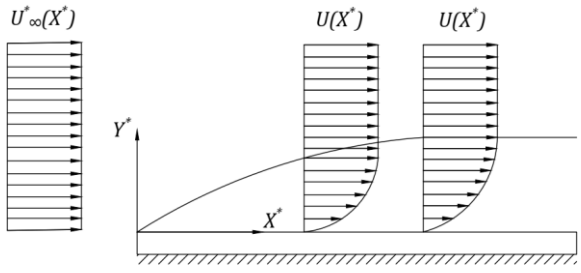

Figure 1. Schematic view of boundary layer flow over a flat plate.

Before embarking on the study's theoretical aspects, let us introduce a schematic description of the problem through Figure 1. As shown in the representation, an incompressible stream is of a uniform velocity profile until it reaches the motionless plate. As soon as the flow is in contact with the plate, the pioneer fluid layer takes its velocity, namely zero, due to the slip law. As ascending perpendicular to the plate, the subsequent layers tend to increase their velocity to the free stream velocity relative to the subjacent layer. Along the plate's length, the spatial distribution of points where fluid layers already acquire the free stream velocity carves out the momentum boundary layer in Figure 1. Note that the thermal part of the sketch is to be described before deriving the energy equation.

2.1 Momentum equations

To determine the velocity profile for an incompressible flow, first, we give the tensorial form of Cauchy momentum equation regardless of the coordinate system and fluid model as below,

$$\rho \mathbf{v}.\nabla\mathbf{v} = -\nabla P^* - \nabla.\boldsymbol{\tau} \tag{3}$$

where ρ is the density, $\mathbf{v}$ is the vectoral velocity, ∇P^* is the pressure gradient and $\boldsymbol{\tau}$ is the stress tensor specific to the fluid type. Accordingly, continuity equation is:

$$\nabla.\mathbf{v} = 0 \tag{4}$$

which holds for compressible flows. In cartesian coordinates, Equation (3) turn out to be,

$$\rho\left(u^*\frac{\partial u^*}{\partial X^*}+v^*\frac{\partial u^*}{\partial Y^*}\right)=\frac{\partial P^*}{\partial X^*}+\frac{\partial}{\partial X^*}\tau_{X^*X^*}+\frac{\partial}{\partial Y^*}\tau_{X^*Y^*} \tag{5}$$

$$\rho\left(u^*\frac{\partial v^*}{\partial X^*}+v^*\frac{\partial v^*}{\partial Y^*}\right)=\frac{\partial P^*}{\partial Y^*}+\frac{\partial}{\partial X^*}\tau_{X^*Y^*}+\frac{\partial}{\partial Y^*}\tau_{Y^*Y^*} \tag{6}$$

for X^* and Y^* momentum, respectively, and Equation (4) is simply:

$$\frac{\partial u^*}{\partial X^*}+\frac{\partial v^*}{\partial Y^*}=0 \tag{7}$$

One can obtain stress components in momentum equations from Equation (2), accordingly:

$$\tau_{X^*X^*}=2\left(\mu_\infty+(\mu_0-\mu_\infty)\left(1+\lambda^m\left(2\left(\frac{\partial u^*}{\partial X^*}\right)^2+2\left(\frac{\partial v^*}{\partial Y^*}\right)^2+\left(\frac{\partial u^*}{\partial Y^*}+\frac{\partial v^*}{\partial X^*}\right)^2\right)^{\frac{m}{2}}\right)^{\frac{n-1}{m}}\right)\frac{\partial u^*}{\partial X^*} \tag{8}$$

$$\tau_{X^*Y^*}=\left(\mu_\infty+(\mu_0-\mu_\infty)\left(1+\lambda^m\left(2\left(\frac{\partial u^*}{\partial X^*}\right)^2+2\left(\frac{\partial v^*}{\partial Y^*}\right)^2+\left(\frac{\partial u^*}{\partial Y^*}+\frac{\partial v^*}{\partial X^*}\right)^2\right)^{\frac{m}{2}}\right)^{\frac{n-1}{m}}\right)\left(\frac{\partial v^*}{\partial X^*}+\frac{\partial u^*}{\partial Y^*}\right) \tag{9}$$

$$\tau_{Y^*Y^*}=2\left(\mu_\infty+(\mu_0-\mu_\infty)\left(1+\lambda^m\left(2\left(\frac{\partial u^*}{\partial X^*}\right)^2+2\left(\frac{\partial v^*}{\partial Y^*}\right)^2+\left(\frac{\partial u^*}{\partial Y^*}+\frac{\partial v^*}{\partial X^*}\right)^2\right)^{\frac{m}{2}}\right)^{\frac{n-1}{m}}\right)\frac{\partial v^*}{\partial Y^*} \tag{10}$$

Notice that since stress tensor is inherently symmetric, it is unnecessary to express $\tau_{X^*Y^*}$ above, i.e., $\tau_{X^*Y^*}=\tau_{Y^*X^*}$. Before boundary layer analysis, complete analytical forms of momentum equations follow in the steps of Equation (5-10) except Equation (6). Alternatively, we apply boundary layer assumptions to Equation (5,6) and Equation (8,10) separately instead of exact momentum equations.

2.2 Energy equations

Predicating the plate and free stream at discrete temperatures of T_w^* and T_∞^*, respectively, the fluid's temperature is likely to vary in the vicinity of the surface, referred to as the thermal boundary layer. However, the conservation of energy also applies to this narrow zone. Right then, the energy equation reads

$$u^*\frac{\partial T^*}{\partial X^*}+v^*\frac{\partial T^*}{\partial Y^*}=\frac{k}{\rho c_p}\left(\frac{\partial^2 T^*}{\partial X^{*2}}+\frac{\partial^2 T^*}{\partial Y^{*2}}\right) \tag{11}$$

in which k, ρ and c_p are, in turn, thermal conductivity, density, and specific heat of the fluid. Furthermore, known solid surface and free-stream temperature conditions imposed on Equation (11) are;

$$T^*(X^*,0)=T_w^* \text{ and } T^*(X^*,\infty)=T_\infty^*. \tag{12}$$

3 Boundary layer analysis

One can define the thickness of the boundary layer, i.e., $\delta^*(X^*)$, as a distance from the surface of the plate where fluid achieves %99 of the velocity of the free stream. For convenience, let us assume the thickness is minimal, therefore mathematically speaking, $\delta^*(X^*) \ll 1$. Conventional boundary layer assumptions require following order of magnitude estimates.

$$x^*\sim O(1),\ y^*\sim O(\delta),\ u^*\sim O(1),\ v^*\sim O(\delta) \text{ and } \delta^{*2} << \delta^* << \frac{1}{\delta^*} << \frac{1}{\delta^{*2}} \tag{13}$$

Following above relations, retaining the highest order terms, the x-momentum equation then reads:

$$\rho\left(u^*\frac{\partial u^*}{\partial X^*}+v^*\frac{\partial u^*}{\partial Y^*}\right)=\frac{\partial P^*}{\partial X^*}+\frac{\partial}{\partial Y^*}\tau_{X^*Y^*} \tag{14}$$

Invoking the same estimates, Equation (9) reduces to;

$$\tau_{X^*Y^*}=\left(\mu_\infty+(\mu_0-\mu_\infty)\left(1+\lambda^m\left(\frac{\partial u^*}{\partial Y^*}\right)^m\right)^{\frac{n-1}{m}}\right)\frac{\partial u^*}{\partial Y^*} \tag{15}$$

Since the initial viscosity is greater than limit viscosity for shear thinning fluids, i.e., $\mu_0 \gg \mu_\infty$, we can disregard μ_∞ from above by comparison with μ_0. Substituting Equation (15) into Equation (14), one can obtains the x-momentum equation in a reduced form as follows:

$$\rho\left(u^*\frac{\partial u^*}{\partial X^*}+v^*\frac{\partial u^*}{\partial Y^*}\right)=-\frac{\partial P^*}{\partial X^*}+\mu_0\left(1+\lambda^m\left(\frac{\partial u^*}{\partial Y^*}\right)^m\right)^{\frac{n-1}{m}}\frac{\partial^2 u^*}{\partial Y^{*2}}+\mu_0\lambda^m(n-1)\left(1+\lambda^m\left(\frac{\partial u^*}{\partial Y^*}\right)^m\right)^{\frac{n-m2-1}{m}}\left(\frac{\partial u^*}{\partial Y^*}\right)^m\frac{\partial^2 u^*}{\partial Y^{*2}} \quad (16)$$

Notice that μ_0 and λ have to be of order $\delta^{*2}$and δ^{*m} respectively to retain terms except those of viscous. The dimensionless variables and parameters can be defined as follows.

$$u=\frac{u^*}{V},v=\frac{v^*}{V},X=\frac{\rho V}{\mu_0}X^*,Y=\frac{\rho V}{\mu_0}Y^*,P=\frac{P^*}{\rho V^2}\text{ and }U_\infty=\frac{U_\infty^*}{V} \quad (17)$$

where V is the reference velocity related to the free stream velocity U_∞^*. Substituting new variables into Equation (16) and rearranging terms to be dimensionless, the x-momentum equation reads,

$$u\frac{\partial u}{\partial X}+v\frac{\partial u}{\partial Y}=-\frac{\partial P}{\partial X}+\left(1+\left(De\frac{\partial u}{\partial Y}\right)^m\right)^{\frac{n-1}{m}}\left(1+(n-1)\frac{\left(De\frac{\partial u}{\partial Y}\right)^m}{1+\left(De\frac{\partial u}{\partial Y}\right)^m}\right)\frac{\partial^2 u}{\partial Y^2} \quad (18)$$

in which $De=\lambda\rho V^2/\mu_0$ is referred to the Deborah number that withstands non-Newtonian behavior. Keeping in mind that $\mu_0\sim O(\delta^{*2})$ and $\lambda\sim O(\delta^{*m})$ as well as considering Equation (13), y-momentum therefore turns out to be:

$$\frac{\partial P}{\partial Y}=0 \quad (19)$$

which indicates $P=P(X)$. Thus, the pressure distribution outside the boundary layer is calculated by the potential theory for the inviscid free stream as follows:

$$P=-\frac{1}{2}U^2+\text{constant} \quad (20)$$

We obtain pressure gradient involved in Equation (18) by deriving Equation (20) with respect to X,

$$\frac{dP}{dX}=-U\frac{dU}{dx} \quad (21)$$

Substituting preceding into Equation (18) yields the final form of the boundary layer equation of Carreau-Yasuda fluid as below:

$$u\frac{\partial u}{\partial X}+v\frac{\partial u}{\partial Y}=U\frac{dU}{dx}+\left(1+\left(De\frac{\partial u}{\partial Y}\right)^m\right)^{\frac{n-1}{m}}\left(1+(n-1)\frac{\left(De\frac{\partial u}{\partial Y}\right)^m}{1+\left(De\frac{\partial u}{\partial Y}\right)^m}\right)\frac{\partial^2 u}{\partial Y^2} \quad (22)$$

subjected to following non-dimensional boundary conditions;

$$u(X,0)=v(X,0)=0,\ u(X,\infty)=U\text{ and }\frac{\partial u}{\partial Y}(X,\infty)=0 \quad (23)$$

The total drag force exerted by fluid to the plate is attributed to the shear stress experienced by the surface. In non-dimensional form, the appropriate shear stress component given in Equation (15) is accordingly is set to the surface as below.

$$\tau_{XY}=\left(1+\left(De\frac{\partial u}{\partial Y}(0)\right)^m\right)^{\frac{n-1}{m}}\frac{\partial u}{\partial Y}(0) \quad (24)$$

In a similar fashion, boundary layer assumptions simplify the energy equation in non-dimensional form to,

$$\frac{u}{r(X)}\frac{\partial}{\partial X}\left(r(X)T\right)+v\frac{\partial T}{\partial Y}=\Pr^{-1}\frac{\partial^2 T}{\partial Y^2} \quad (25)$$

where $Pr=c_p\mu_0/k$ is the Prandtl number. The dimensionless temperature is defined as;

$$T=\left(\frac{T^*-T_\infty^*}{T_w^*-T_\infty^*}\right)\frac{1}{r(X)} \quad (26)$$

in which $r(X)$ is deliberately assigned to the denominator to transform boundary conditions with success and to be acquired in an analytical form later. The boundary conditions are written dimensionless as

$$T(X,0)=\frac{1}{r(X)}\text{ and }T(X,\infty)=0 \quad (27)$$

By now, we have the momentum and thermal boundary layer equations in partial differential equation forms, about which a thorough search of the relevant literature did not yield any related article on Carreau-Yasuda fluid. Thus, the equations have, to the best of the authors' knowledge, not been presented in literature before.

4 Symmetries of the boundary layer equations

A set of transformations that remains an equation invariant is a type of symmetry in an algebraic manner. The existence of such symmetries may lead us to success in solutions of the differential equation. Using the symmetries, in essence, as a set of transformations belonging to a partial differential equation, a reduction to an ordinary form is quite possible. Lie groups and their algebra overcome the problems associated with finding out fundamental symmetries that a differential equation accepts. For the details of the theory, please refer to Bluman and Kumei [14]. Considering the findings, equations arising from boundary layer flows admit several transformations for the symmetries, such as scaling and translational [18]. As was just pointed out, we only consider scaling symmetries to adopt the equations and, hence, define the following new variables as;

$$\bar{x}=e^{-\alpha_1}x,\bar{y}=e^{-\alpha_2}y,\bar{u}=e^{-\alpha_3}u,\bar{v}=e^{-\alpha_4}v,\bar{U}=e^{-\alpha_5}U,\bar{T}=e^{-\alpha_6}T,\ \bar{r}=e^{-\alpha_7}r \quad (28)$$

In terms of the above variables, momentum, continuity, and energy equations, in turn, are

$$\bar{u}\frac{\partial\bar{u}}{\partial\bar{x}}+e^{-\alpha_3+\alpha_1+\alpha_4-\alpha_2}\bar{v}\frac{\partial\bar{u}}{\partial\bar{y}}=e^{-2\alpha_5-2\alpha_3}\bar{U}\frac{\partial\bar{U}}{\partial\bar{x}}+e^{-\alpha_3-2\alpha_2+\alpha_1}\frac{\partial^2\bar{u}}{\partial\bar{y}^2}$$
$$\left(1+\left(e^{\alpha_3-\alpha_2}De\frac{\partial\bar{u}}{\partial\bar{y}}\right)^m\right)^{\frac{n-1}{m}}\left(1+(n-1)\frac{\left(e^{\alpha_3-\alpha_2}De\frac{\partial\bar{u}}{\partial\bar{y}}\right)^m}{1+\left(e^{\alpha_3-\alpha_2}De\frac{\partial\bar{u}}{\partial\bar{y}}\right)^m}\right),\quad(29)$$
$$\frac{\partial\bar{u}}{\partial\bar{x}}+e^{\alpha_1-\alpha_3+\alpha_4-\alpha_2}\frac{\partial\bar{v}}{\partial\bar{y}}=0,$$
$$\frac{\bar{u}}{\bar{r}(\bar{x})}\frac{\partial}{\partial\bar{x}}\left(\bar{r}(\bar{x})\bar{T}\right)+e^{-\alpha_3+\alpha_1+\alpha_4-\alpha_2}\bar{v}\frac{\partial\bar{T}}{\partial\bar{y}}=Pr^{-1}e^{-2\alpha_2-\alpha_3+\alpha_1}\frac{\partial^2\bar{T}}{\partial\bar{y}^2}$$

from which we extract the following equations leaving the original equations invariant.

$$\begin{aligned}\alpha_1-\alpha_3+\alpha_4-\alpha_2&=0,\\-2\alpha_3+2\alpha_5&=0,\\\alpha_1-2\alpha_2-\alpha_3&=0,\\\alpha_3-\alpha_2&=0.\end{aligned}\quad(30)$$

Notice that all parameters can be found in terms of α_3, whereas α_6 and α_7 are arbitrary due to lack of equations depending on them. Thus, the invariance holds if and only if,

$$\begin{aligned}\alpha_1&=3\alpha_3,\\\alpha_2&=\alpha_3,\\\alpha_4&=-\alpha_3,\end{aligned}\quad(31)$$

regardless of α_6 and α_7. Setting $\alpha_6=1$ and remaining α_7 as itself, the associated equations which yield similarity variable and functions are;

$$\frac{dx}{3x}=\frac{dy}{y}=\frac{du}{u}=\frac{dv}{-v}=\frac{dU}{U}=\frac{dT}{T}=\frac{dr}{\alpha_7 r}.\quad(32)$$

Stepwise integration of the system leads to the similarity variable and functions,

$$\xi=x^{-1/3}y,\ f(\xi)=x^{-1/3}u,\ g(\xi)=x^{1/3}v,\ h(\xi)=x^{-1/3}U,\ z(\xi)=x^{-1/3}T,$$
$$w(\xi)=x^{-\alpha_7/3}r.\quad(33)$$

which are expected to transform the governing equations into ordinary form. The transformation is achieved by ultimate equations in which, except similarity variables, originals are anticipated to vanish, and of course, in boundary conditions. Although comparatively tedious calculations emerge from partial differential equations, similarity transformations usually collapse due to boundary conditions. Therefore, before getting into equations, here we unconventionally exploit the reference velocity V and arbitrary constant α_7 to overcome our case. For instance, the third condition in Equation (23) is equivalent to,

$$f(\infty)=x^{-1/3}U\quad(34)$$

in which presenting the term of $x^{-1/3}$ associated with original variables is inconvenient for a complete transformation. To discard it, recalling the dimensionless stream velocity as $U=U^*/V$ and defining $V=x^{-1/3}U^*$ yield

$$f(\infty)=1.\quad(35)$$

Fortunately, the remaining conditions in Equation (23) are not alike the previous, that is,

$$f(0)=0,\ g(0)=0,\ f'(\infty)=0.\quad(36)$$

In the following, we treat analogously the first condition in Equation (23)

$$z(0)=\frac{x^{-1/3}}{r(X)}\quad(37)$$

where $r(x)=w(\xi)x^{\alpha_7/3}$ as seen from Equation (33). By the definition of dimensionless temperature given in Equation (27), $r(x)$ must depend only on x, i.e., $r=r(x)$; nevertheless, the dependence of y arises from the similarity function $w=w(\xi)$ and variable $\xi=\xi(x,y)$. There is no objection to assume $w(\xi)$ as an arbitrary constant, so that $r(x)=x^{\alpha_7/3}$ provided by $w(\xi)=1$, since the preceding assumption that the similarity function $h(\xi)$ is assigned to 1 is fundamentally adequate. Note that it is analogously admissible for similarity function $h=h(\xi)$ to assume $h=1$. Returning to Equation (37), it now follows that,

$$z(0)=1\quad(38)$$

by setting $\alpha_7=1$. Enforcing the similarity variables for the latter in Equation (27), we have

$$z(\infty)=0.\quad(39)$$

In the light of previous results so far, substituting similarity variables and functions into, in turn, continuity, momentum, and thermal boundary layer equations yields

$$\begin{aligned}&f-\xi f'+3g'=0,\\&f^2-\xi ff'+3gf'=1+3f''(1+(De\,f')^m)^{\frac{n-1}{m}}\left(1+\tfrac{(n-1)(De\,f')^m}{1+(De\,f')^m}\right),\\&z''+\Pr\left(\frac{\xi f}{3}-g\right)z'=0\end{aligned}\quad(40)$$

which are subjected to six boundary conditions given in Equations (35), (36), (38) and (39). Consequently, equivalence of shear stress in terms of similarity functions is

$$\tau_{xy}=\left(1+(Def'(0))^m\right)^{\frac{n-1}{m}}f'(0)\quad(41)$$

and similarly, Nusselt number turns out to be;

$$Nu=-Re\,z'(0).\quad(42)$$

Scaling horizontal velocity and axis with $\sqrt{Re}$ in Equation (17) leads that $\sqrt{Re}\,De$ arises as a modified Weissenberg number instead of Deborah number in the rest from Equation (18). Therefore, the Nusselt number can also be calculated using $Nu=-\sqrt{Re}\,z'(0)$ instead of Equation (42). In the

next chapter, we focus on a numerical procedure for the system of differential equations given in Equation (40).

5 Numerical analysis

Since the system of differential equations is highly nonlinear and coupled, exact solutions are presumably not tractable. Exploiting numerical approaches are, therefore, more useful for such systems, despite the need for higher computational labor. In order to handle a system of differential equations numerically, it is common to convert them into a first-order system in advance. Here, we start by introducing following variables;

$$f = f_1, f' = f_2, g = f_3, z = f_4, z' = f_5. \tag{43}$$

Together with solving the highest order terms from Equation (40) in terms of above variables, the first order derivatives constitute the system in question as follows,

$$\begin{aligned} f_1' &= f_2, \\ f_2' &= \left(f_1^2 - \xi f_1 f_2 + 3 f_3 f_2 - 1\right) \Big/ \left(3\left(1+\left(De\, f_2\right)^m\right)^{\frac{n-1}{m}} \left(1+\frac{(n-1)(De\, f_2)^m}{1+(De\, f_2)^m}\right)\right), \\ f_3' &= \left(f_1 - \xi f_2\right)/-3, \\ f_4' &= f_5, \\ f_5' &= De\, f_5 \left(f_3 - \xi f_1/3\right) \end{aligned} \tag{44}$$

subject to,

$$f_1(0)=0,\ f_1(\infty)=1,\ f_3(0)=0,\ f_4(0)=1,\ f_4(\infty)=0. \tag{45}$$

In general, finite difference schemes in which differential equations are transformed to a system of algebraic equations are employed for boundary value problems, such as boundary layer equations. For the purpose of achieving numerical solutions of the system given in Equation (44), we utilize a MATLAB subroutine, i.e., bcp4c, implementing finite difference technique with adaptive mesh refinement by collocation polynomials. The numerical procedure accomplishes when the relative error tolerance of 10^{-6} is met.

6 Results and discussions

In this chapter, to feature primarily non-Newtonian effects on the boundary layer flow, the results are provided in detail through figures plotted via the numerical data. It should be emphasized here that since the boundary layer originates substantially from the horizontal velocity, we only discuss the alterations over first similarity functions related to that, namely f.

Variations of f the similarity function with increasing Deborah number are shown in Figure 2. The boundary layer undergoes thickening for an increase in Deborah number, which indicates slower fluid velocity. More simply, when a large Deborah number presents, the fluid tends to be solid-like

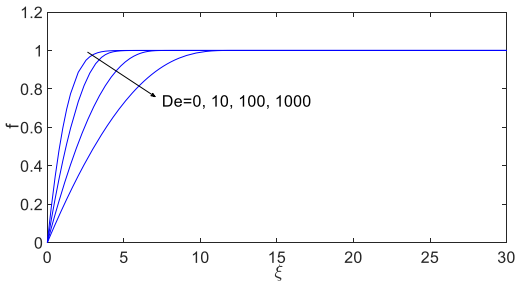

Figure 2. Variations of similarity function $\boldsymbol{f}$ related to horizontal component of the velocity for various Deborah numbers ($\boldsymbol{n = 1.5}$ and $\boldsymbol{m = 2}$).

In Figure 3, the effect of the power-law index $\boldsymbol{n}$ on the same similarity function is depicted. Analogous to Deborah number, giving an increase in $\boldsymbol{n}$ triggers retardation in the overall fluid velocity and consequently leads to a thicker boundary layer. It may be noted from the figure that while descending the Newtonian case, i.e., $n < 1$ related to shear thinning, resistance to flow diminishes as well, thus a thinner boundary layer is manifest.

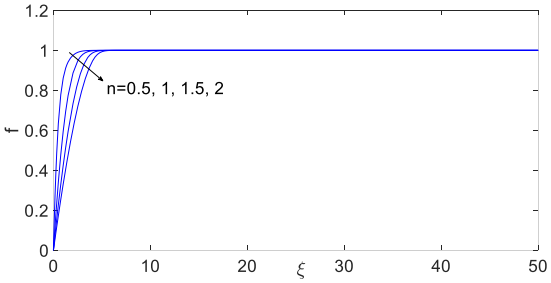

Figure 3. Variations of similarity function $\boldsymbol{f}$ related to the horizontal component of the velocity for various primary power-law index $\boldsymbol{n}$ ($\boldsymbol{De = 10}$ and $\boldsymbol{m = 2}$).

For the last in the debate of the momentum boundary layer, we devote Figure 4 to the alteration of f with the denominator index peculiar to the fluid model, i.e., m. As seen from the figure, m manifestly takes a contrariwise role to n in the alteration; however, as values grow, its effect progressively diminishes. Note that as $m \to \infty$, the fluid behaves more like a Newton fluid.

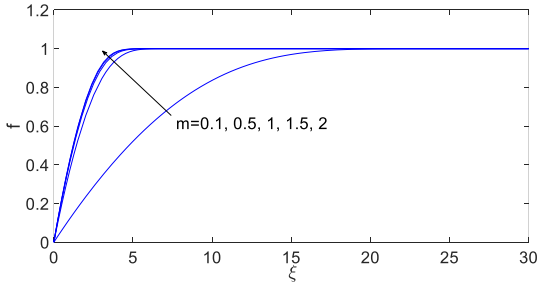

Figure 4. Variations of similarity function f related to the horizontal component of the velocity for various secondary power-law index m ($De = 10$ and $n = 1.5$).

Figure 5 depicts z the similarity function related to the fluid temperature as a function of ξ for various Deborah numbers. Following the figure, a fluid with slower velocity due to an increasing Deborah number has a higher temperature over a warmer flat plate since the convection becomes less forced. In contrast, the heat transfer between the fluid and the warmer plate enhances as the fluid gains speed at lower Deborah numbers.

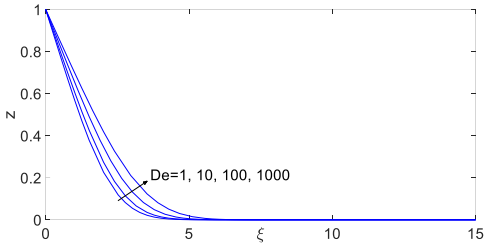

Figure 5. Variations of similarity function z related to the temperature of the fluid for various Deborah numbers ($n = 1.5$, $m = 2$ and $Pr = 1$).

In the same manner, the power-law constants, i.e., n and m, alter fluid temperature implicitly over fluid velocity, as seen from Figure 6 and Figure 7. The fluid thickens and slows down with increasing n or equivalently decreasing m and becomes warmer as a result of less effective forced convection.

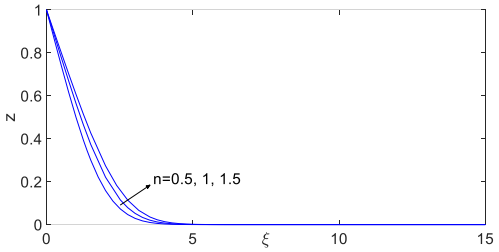

Figure 6. Variations of similarity function z related to the temperature of the fluid for various power-law index n ($De = 10, m = 2$, and , $Pr = 1$).

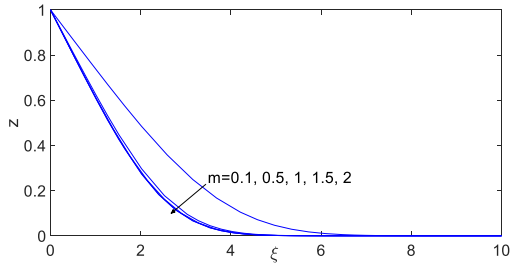

Figure 7. Variations of similarity function z related to the temperature of the fluid for various secondary power-law index m ($De = 10$, $n = 1.5$ and $Pr = 1$).

It is also convenient to employ the Prandtl number to determine whether the heat transfer is dominated by convection or conduction through the fluid motion. For a boundary layer flow, the Prandtl number, widely regarded as the ratio of momentum diffusivity to thermal diffusivity, compares the thickness of momentum and thermal boundary layers. Thus, for various Prandtl number values, the curves of z versus ξ are plotted in Figure 8. Decreasing Prandtl number indicates that conduction becomes more critical than convection, plus shrinking the thermal boundary layer thickness. Contrarily, momentum diffusivity dominates total heat transfer, which triggers smaller temperature gradients within a thicker thermal boundary layer.

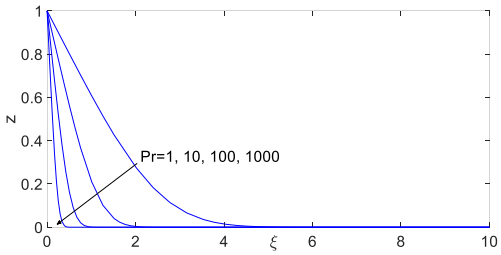

Figure 8. Variations of similarity function z related to the temperature of the fluid for various Prandtl number ($De = 10$, $n = 1.5$ and $Pr = 1$).

In seeking more in-depth insight into the convection and the rate of heat transfer, we plotted the Nusselt number as a function of Deborah number for several values of n in Figure 9. The Nusselt number is, in brief, a measure of the enhancement of heat transfer by convection relative to conduction, and therefore implies the improvement of convective heat transfer for increasing values. From Figure 9, one can observe three distinct characteristics concerning n values of Nusselt versus Deborah curves. For $n = 1$, which extinguishes the Deborah number entirely in the governing equations and corresponds to Newtonian fluid, the Nusselt number becomes constant of a value of 4.5. For $n = 1.5$ associated with a shear thickening fluid, from a value of 4.5 at $De = 0$, the Nusselt number decreases asymptotically to a value of 3.45 for an increasing Deborah number. However, for $n = 0.5$ associated with a shear-thinning fluid, the heat transfer by convection becomes elevated by increasing the Nusselt number, even though Deborah number increases considerably.

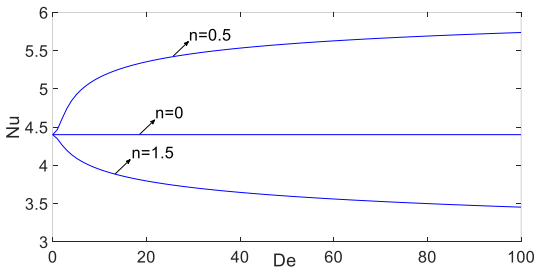

Figure 9. The Nusselt number curves as a function of the Deborah number for various primary power-law index n ($Re = 10$, $m = 2$and $Pr = 1$).

Since it is also of interest to examine how the Nusselt number can vary with the Prandtl number and m, Figure 10 is plotted. Unlike n, increasing m makes fluid thinner, which leads Nusselt number to increase as would be expected. Furthermore, from the figure, we infer that as the Prandtl number increases, the flow becomes more convective compared to the conduction, which gives the Nusselt number rise.

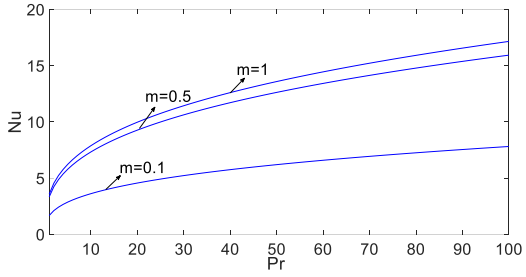

Figure 10. The Nusselt number curves as a function of the Prandtl number for various secondary power-law index m ($Re = 10$, $n = 2$ and $De = 10$).

Relying on Equation (41), Figure 11 depicts the non-dimensional shear stress varying with Deborah number for various n values. As seen from the figure, the friction force that is merely exerted by shear thickening fluids, i.e., n in excess of 1, grows while both De and n increase. For a shear-thinning fluid of $n = 0.5$, conversely, the friction force associated with shear stress on the surface reduces asymptotically as Deborah number increases. Even though fluids considered in the figure are mere shear-thinning, we must state that a shear-thickening fluid responds contrariwise as Deborah number increases. However, the response of shear stress acts reversely for increasing m values which diminish the apparent viscosity, as seen from Figure 12.

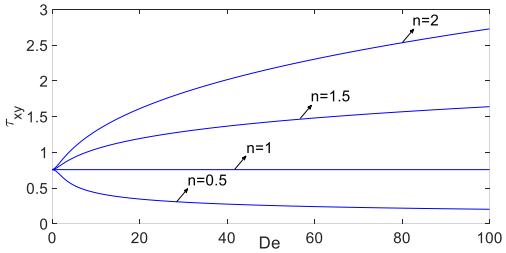

Figure 11. The shear stress curves as a function of the Deborah number for various power-law index n ($Re = 10$, $m = 2$ and $Pr = 1$)

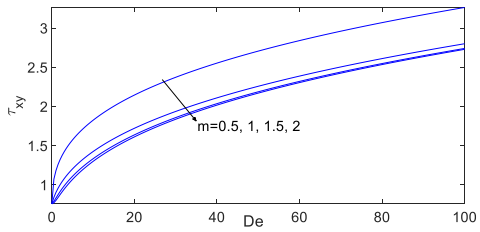

Figure 12. The shear stress curves as a function of the Deborah number for various secondary power-law index m ($Re = 10$, $n = 2$ and $Pr = 1$).

7 Conclusions

The present study rests on the boundary layer theory renowned for its simplifying but realistic assumptions in studies of external viscous flows. The flow concerning a non-Newtonian fluid is accordingly over a flat plate and induced by a free stream and being steady besides. The free stream is regarded as an inviscid flow with uniform velocity, except the flow inside the boundary layer overlies the plate. For the rest of the governing equations, we assigned the Carreau-Yasuda model to non-Newtonian fluid because of its capability to predict varying viscosity decently within the broadest possible range of deformation rates. To examine the fluid's thermal attributes, we also introduced a temperature difference between the motionless plate and the upcoming stream to initiate the heat transfer. Thus, the temperature of the fluid varies solely within the thermal boundary layer analogous to that of momentum, which is coupled with the conservation of energy. Momentum and thermal boundary layer equations were derived in partial differential form; however, later solved numerically in ordinary form thanks to similarity transformations. Therefore, solutions of similarity variables related to velocity and temperature profiles were illustrated for varying convenient nondimensional parameters, such as Deborah and Prandtl numbers. To inquire how effectively convective heat transfer takes place, we carried through an investigation based on the Nusselt number. The force that a fluid exerts a solid body in external flows is of engineering interest; accordingly, the shear stress at the surface was presented in depictions for various dimensionless parameters.

To conclude, we briefly review the key results emphasized throughout the paper as follows.

- Increasing Deborah number gives a decrease to the fluid velocity, consequently resulting in thickening in the momentum boundary layer.
- When $n > 1$ belongs to shear thickening fluids, the fluid behaves more like a solid in a way that the momentum boundary layer thickens.
- Unlike n, increasing the secondary power-law index, i.e. m, that occupies in the denominator peculiar to the Carreau-Yasuda model, accelerates the fluid in a way that the momentum boundary layer gets thinner.
- Fluids at great Deborah numbers are in higher temperatures than those with less, requiring a thicker thermal boundary layer.
- An effect that facilitates the flow, for instance, decreasing n or controversially increasing m, reduces the fluid temperature, and narrows the thermal boundary layer.
- For small Prandtl numbers, especially $Pr < 1$, the heat transfer across the fluid layers is mainly via conduction, resulting in higher fluid temperature and a thicker thermal boundary layer.
- Relying on variations of the Nusselt number, the convection enhances throughout a shear-thinning fluid by increasing Deborah number, whereas an

increase alike counterworks in a shear-thickening fluid.

- When $Pr \gg 1$, heat transfer by momentum diffusivity, i.e., convection, dominates relative to thermal diffusion, i.e., conduction. This fact also exposes the Nusselt number increases as long as the Prandtl number increase in such flows.
- Increasing the Deborah numbers leads to growing shear stress, which a shear thickening fluid exerts on the plate. However, concerning a shear-thinning fluid, shear stress decreases as the Deborah number increase.

We here concluded that the Carreau-Yasuda model is highly capable of mathematically representing a diverse range of non-Newtonian fluids at the expense of intense calculation labor.

Conflict of interest

The authors declare that there is no conflict of interest.

Similarity Index (iThenticate): 6%

References

[1] F. A. Morrison, Understanding Rheology. Oxford University Press, New York ABD, 2001.

[2] H. Ozoe and Stuart W. Churchill, Hydrodynamic stability and natural convection in Ostwald-de Waele and Ellis fluids: The development of a numerical solution, AIChE Journal, 18(6), 1196-1207, 1972. https://doi.org/10.1002/aic.690180617

[3] M. M. Cross, Rheology of non-newtonian fluids: a new flow equation for pseudoplastic systems, Journal of Colloid Science, 20(5), 417-437, 1965. https://doi.org/10.1016/0095-8522(65)90022-X

[4] A. M. Siddiqui, M. Ahmed and Q. K. Ghori, Couette and Poiseuille flows for non-Newtonian fluids, International Journal of Nonlinear Sciences and Numerical Simulation, 7(1), 15-26,2006. https://doi.org/ 10.1515/IJNSNS.2006.7.1.15

[5] K. Khellaf and G. Lauriat, Numerical study of heat transfer in a non-Newtonian Carreau-fluid between rotating concentric vertical cylinders, Journal of non-Newtonian Fluid Mechanic, 89, 45-61, 2000. https://doi.org/10.1016/S0377-020257(99)0030-0

[6] I. Lashgari, J. O. Pralits, F. Giannetti and L. Brandt, First instability of the flow of shear-thinning and shear thickening fluids past a cylinder, Journal of Fluid Mechanics, 701, 201-227, 2012. https://doi.org/10.1017/jfm.2012.151

[7] F. M. Abbasi, T. Hayat and A. Alsaedi, Numerical analysis for MHD peristaltic transport of Carreau–Yasuda fluid in a curved channel with Hall effects, Journal of Magnetism and Magnetic Materials, 382, 104-110, 2015. https://doi.org/10.1016/j.jmmm.2015.01.040

[8] J. Boyd, M. J. Buick and S. Green, Analysis of the Casson and Carreau-Yasuda non-Newtonian blood models in steady and oscillatory flow using the lattice Boltzmann method, Physics of Fluids, 19,093103,2007. https://doi.org/10.1063/1.2772250

[9] K. V. S. N. Raju, D. Krishna, G. Rama Devi, P. J. Reddy and M. Yaseen, Assessment of applicability of Carreau, Ellis, and Cross models to the viscosity data of resin solutions, Journal of Applied Polymer Science, 48, 2101-2112, 1993. https://doi.org/10.1002/app.1993.070481205

[10] J. Koszkul and J. Nabialek, Viscosity models in simulation of the filling stage of the injection molding process, Journal of Materials Processing Technology, 157-158, 183-187, 2004. https://doi.org/10.1016/j.jmatprotec.2004.09.027

[11] H. Schlichting, Boundary Layer Theory McGraw-Hill. New York, ABD, 1979.

[12] A. Pantokratoras, Non-similar Blasius and Sakiadis flow of a non-Newtonian Carreau fluid, Journal of the Taiwan Institute of Chemical Engineers, 56, 1-5, 2015. https://doi.org/10.1016/j.jtice.2015.03.021

[13] M. Khan and A. Hashim, Boundary layer flow and heat transfer to Carreau fluid over a nonlinear stretching sheet, AIP Advances, 5(10), 107203, 2015. https://doi.org/10.1063/1.4932627

[14] G. W. Bluman and S. Kumei, Symmetries and Differential Equations. Springer Science & Business Media, 2013.

[15] Y. Aksoy, T. Hayat and M. Pakdemirli, Boundary layer theory and symmetry analysis of a Williamson fluid, Zeitschrift für Naturforschung, 67(6-7), 363-368, 2012. https://doi.org/10.5560/zna.2012-0028

[16] G. Sarı, M. Pakdemirli, T. Hayat and Y. Aksoy, Boundary layer equations and Lie group analysis of a Sisko Fluid, Journal of Applied Mathematics, 2012, 259608, 2012. https://doi:10.1155/2012/259608

[17] T. Hayat, M. Pakdemirli and Y. Aksoy, Similarity solutions for boundary layer equations of a Powel-eyring fluid, Mathematical and Computational Applications, 18(1), 62-70, 2013. https://doi.org/10.3390/mca18010062

[18] M. Yürüsoy and M. Pakdemirli, Group classification of a non-Newtonian fluid model using classical approach and equivalence transformations, International Journal of Non-Linear Mechanics, 34(2), 341-346, 1999. https://doi.org/10.1016/S0020-7462(98)00037-7